



Towards control in Suzuki-Miyaura CTCP – the synergy between water and RuPhos

Siebe Detavernier^a, Florian Matz^b, Julien De Winter^c, Pascal Gerbaux^c, Thomas-C. Jagau^b, Guy Koeckelberghs^{a,*}

^a Laboratory for Polymer Synthesis, KU Leuven, Celestijnenlaan 200F – box 2404, B-3001 Heverlee, Belgium

^b Quantum Chemistry and Physical Chemistry, KU Leuven, Celestijnenlaan 200F, B-3001 Heverlee, Belgium

^c Organic Synthesis and Mass Spectrometry Laboratory, Center of Innovation and Research in Materials and Polymers (CIRMAP) – University of Mons (UMONS), Place du Parc 23, B-7000 Mons, Belgium

ARTICLE INFO

Keywords:

Conjugated Polymers
Suzuki-Miyaura CTCP
Controlled Polymerization
Pd(RuPhos)
External Initiators

ABSTRACT

Pd(RuPhos) has recently been introduced as an external initiator for Suzuki-Miyaura catalyst transfer condensative polymerizations (SMCTCPs), exhibiting a controlled polymerization behavior. Paradoxically, the same initiator also enables a controlled activation-deactivation polymerization, raising questions about how these opposing mechanisms can yield controlled polymerizations. This study investigates key parameters influencing control in SMCTCP using poly(3-hexylthiophene) (P3HT), synthesized with a bench-stable, isolated external Pd (RuPhos) initiator, thereby elucidating why these two mechanisms can result in a controlled polymerization behavior. Our results demonstrate that increasing the water content reduces chain transfer reactions in the presence of a chain transfer agent (CTA). Alternative cosolvents, including 1-hexanol and anisole, are explored to mitigate water's other adverse effects, showing a similar beneficial impact, though complete control remains challenging. Introducing additional RuPhos significantly reduces transfer reactions, producing P3HT with a dispersity of 1.16 compared to 1.28 without additional ligand, indicating improved control even with CTA present. The controlled nature of the polymerization is further validated through ¹H NMR and MALDI-ToF analyses. A ³¹P NMR study reveals that free RuPhos forms in the absence of additional ligand, compromising control during polymerization. A computational survey of the coordination environment of the catalytic palladium species and the measurement of reaction rates strongly suggest that water and RuPhos act synergistically: water stabilizes the Pd(RuPhos)-polymer complex via a solvent cage, while additional RuPhos prevents diffusion of the Pd(RuPhos) complex. These findings reconcile the disparate mechanisms of SMCTCP and activation-deactivation polymerization, highlighting the critical roles of water and RuPhos in controlling transfer reactions.

1. Introduction

Conjugated polymers (CPs) represent a cornerstone of modern materials science, holding immense promise across a spectrum of applications from optoelectronics to biomedicine [1–7]. Tailoring these polymers in order to meet specific application requirements encompasses considerations ranging from fundamental parameters as monomer selection to nuanced characteristics such as the degree of polymerization (DP), the dispersity (Đ) [8], the nature of the end groups [9] and defects [10,11]; all of which profoundly influence material performance [12]. Traditionally, step-growth polymerization has been the route to CP synthesis, but its inherent limitations in parameter

control necessitate more precise methodologies [13]. In response, controlled chain-growth catalyst transfer condensative polymerization (CTCP) has emerged as the preferred approach [14]. Suzuki-Miyaura CTCP (SMCTCP), in particular, enjoys prominence for its versatility, tolerance to diverse functional groups and substrates, low toxicity, and mild reaction conditions, making it indispensable for achieving precise and efficient synthesis of CPs [15–18].

However, despite its virtues, SMCTCP encounters challenges, notably due to the presence of water as a solvent in the reaction mixture. While water aids in solubilizing the base and interacting with the catalyst [19–21], it also limits the solubility of the apolar, organic monomers and conjugated polymers, and it triggers undesirable side

* Corresponding author at: Laboratory for Polymer Synthesis, KU Leuven, Celestijnenlaan 200F, B-3001 Heverlee, Belgium.

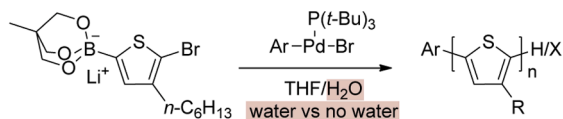
E-mail address: guy.koeckelberghs@kuleuven.be (G. Koeckelberghs).

<https://doi.org/10.1016/j.eurpolymj.2025.113951>

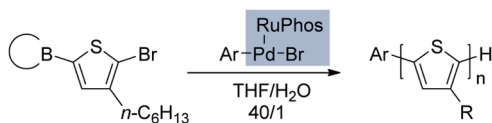
Received 31 January 2025; Received in revised form 7 April 2025; Accepted 14 April 2025

Available online 23 April 2025

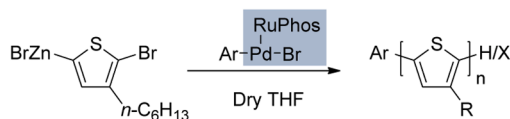
0014-3057/© 2025 Elsevier Ltd. All rights reserved, including those for text and data mining, AI training, and similar technologies.

a) Suzuki-Miyaura CTCP - Yokozawa

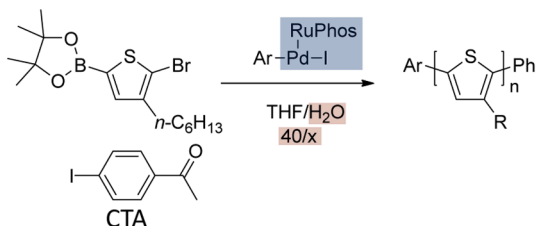
No water = no intramolecular transfer

b) Suzuki-Miyaura CTCP - Choi

Controlled catalyst transfer condensative polymerization
Catalyst stays attached

c) Universal chain-growth polymerization - Koeckelberghs

Activation-deactivation → **Controlled chain-growth**
Catalyst diffuses away

d) Suzuki-Miyaura CTCP - this research

Impact amount of water on transfer reaction
Impact extra ligand on controlled behavior

Fig. 1. Different strategies aiming towards control. a) universal chain-growth polymerization, and b) SMCTCP, both using PdRuPhos as initiator moiety. c) Showing the importance of water in SMCTCP and d) our research investigating the impact of water and RuPhos on the controlled behavior of the SMCTCP.

reactions, such as protodeboronation and dehalogenation. However, Yokozawa *et al.* highlighted the pivotal role of water in SMCTCP as it promotes intramolecular transfer of the Pd catalyst, facilitating a controlled polymerization character (Fig. 1a) [22]. In light of these complexities, the question arises: what further insights can be gleaned into the role of water in SMCTCP?

Recent years have seen a resurgence of interest in Suzuki-Miyaura polymerization for CTCP, particularly due to the work of Choi *et al.*, as they improved the controlled and living character of the polymerization. They demonstrated the synthesis of diverse CPs with low dispersity and high regioregularity using bench-stable Buchwald precatalysts in combination with monomers containing *N*-methylimidodiacetic acid (MIDA) boronate protection groups and derivatives as boron moiety (Fig. 1b) [23,24]. Even with boronic ester monomers, prone to protodeboronation, a controlled polymerization was achieved when targeting a lower degree of polymerization [25]. This controlled process ensures that each initiator molecule initiates a single polymer chain and remains attached throughout the polymerization, reducing transfer and termination side reactions.

Contrastingly, our earlier research using the same Pd(RuPhos) initiator system in a Negishi polycondensation revealed an opposite mechanism (Fig. 1c) [26]. In this system, an isolated (Ar)Pd(RuPhos)-Br species, similar to the *in-situ* generated Pd(RuPhos) initiator from Buchwald precatalysts, facilitated a controlled polymerization via an activation-deactivation process, as introduced by Yokozawa in 2007 [13]. Here, the catalyst *does* dissociate from the polymer chain, but exclusively oxidatively inserts into growing polymer chains, avoiding insertion into the unreacted monomers, thereby maintaining control. This is possible as the reactivity of the C-Br bond in the monomer is reduced due to the deactivating C-Zn bond. In the growing polymer chain, this Zn-C bond is not present and the C-Br bond present at the last monomer unit in the polymer chain is activated [10,27]. Despite the disparate mechanisms — ring walking in SMCTCP and activation-deactivation in this type of Negishi polycondensation — the outcome is the same: a controlled polymerization which underscores the versatility of the catalyst system. However, it also again raises the question of how the same initiator can operate in such opposing manners — staying attached in one case or diffusing away and reinserting in another case.

The mechanistic differences likely stem from variations in the reagents used in SMTCP and Negishi polymerization. Suzuki-Miyaura polymerizations require water, while Negishi polymerizations are conducted under moisture-free conditions. Additionally, the monomers have a different functional group, thereby altering the reactivity and polymerization mechanism. Finally, Choi *et al.* also introduced varying amounts of additional dialkyl biaryl monophosphine ligands, primarily RuPhos, during initiator synthesis, resulting in significantly reduced dispersity for the polymerization of several monomers [23–25,28]. Mechanistically, it would seem unnecessary to add more ligand than the amount of palladium present during the *in-situ* synthesis of the external initiator, as oxidative insertion of an aryl iodide with RuPhos Pd G3 and the following polymerization should not require extra free ligand [29]. However, calculations regarding this SMCTCP mechanism using Pd (RuPhos) initiators have yet to be performed.

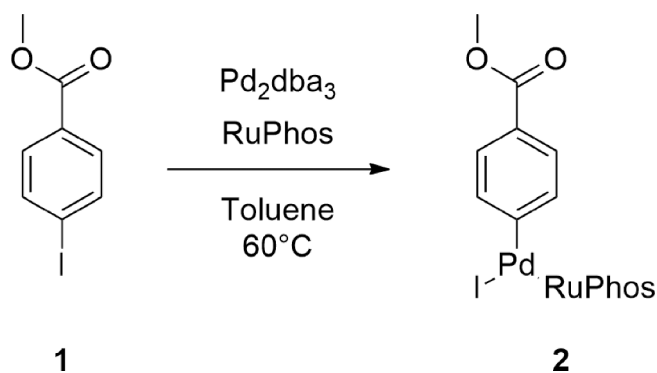
In this study, we aim to unravel the intricate interactions influencing control in SMCTCP, thereby focusing on explaining the paradoxical character between the SMCTCP and the activation-deactivation Negishi polymerization. By isolating the external initiator, control over the initiation step is improved. The effect of the amount of water and RuPhos, and different cosolvents on the molar mass and the dispersity is examined (Fig. 1d). The addition of a chain transfer agent (CTA) further elucidates the controlled character. Furthermore, determining the rate-determining step and reaction rate pinpoints at what point in the catalytic cycle water and RuPhos can affect the polymerization dynamics. These experimental findings are supported by a computational study of the energetics of different coordination environments of the catalytic palladium species, leading to a working hypothesis regarding how RuPhos can affect the controllability of the polymerization.

2. Results and discussion

2.1. Synthesis and isolation of the external initiator

For the synthesis of CPs via SMCTCP, the initiator is typically generated *in-situ*. Over the past decade, various approaches have been explored to enhance the performance of the palladium initiators and catalysts. Currently, the most advanced and controlled polymers utilize RuPhos Pd G3 in combination with aryl iodides to synthesize the external initiator before the initiation of the polymerization [24,25,28,30]. However, the inability to isolate this external initiator poses challenges in monitoring conversion rates, determination of the exact number of active palladium species and control over the end groups. These limitations compromise the controlled nature of the polymerization process to some extent.

To overcome these issues, the use of an isolated external Pd initiator, (Ar)Pd(RuPhos)-iodine, is proposed. This molecule is synthesized from



Scheme 1. Synthesis of the isolated external initiator.

$\text{Pd}_2(\text{dba})_3 \cdot \text{CHCl}_3$ (dba = dibenzylideneacetone), RuPhos, and an aryl halogenide, e.g., 4-iodo-methyl benzoate, which undergoes oxidative insertion and ligand exchange to form the external initiator **2** (Scheme 1). The chloroform adduct of $\text{Pd}_2(\text{dba})_3$ is selected for its higher stability and purity. Following concentration and filtration through celite, the crude product is precipitated using cold pentane. The resulting initiator is characterized using ^1H and ^{31}P NMR and is air-, moisture-, and solution-stable.

2.2. Influence of water on SMCTCPs

As suggested by Yokozawa *et al.*, the presence of water is believed to play a crucial role in promoting intramolecular transfer in SMCTCPs. To explore the relationship between the water concentration and transfer reactions, SMCTCP experiments are conducted using varying ratios of THF to water, while maintaining a constant THF concentration and total volume. In the first series of experiments, 2-bromo-3-hexylthiophene-2-boronic acid pinacol ester **M1**, is polymerized using the isolated external Pd(RuPhos) initiator **2**, with a fixed monomer-to-initiator ratio of 30. The THF/ H_2O ratio varies from 60/1 to 40/1 and 10/1. In a second

series, an additional 20 mol% of a CTA, 4-iodoacetophenone, is added to assess the extent of transfer reactions during the polymerization (Scheme 2). After polymerization, the obtained P3HT is precipitated in methanol and filtered to remove residual monomer and impurities, without removing the low molar mass polymer molecules, as this would otherwise give a distorted view of the actual obtained material. The polymers are characterized using size exclusion chromatography (SEC) and ^1H NMR to compare the dispersity, number average molar mass (\bar{M}_n), end groups, and, importantly, the top of the polymer distribution ($\bar{M}_{n,\text{top}}$), among the different samples.

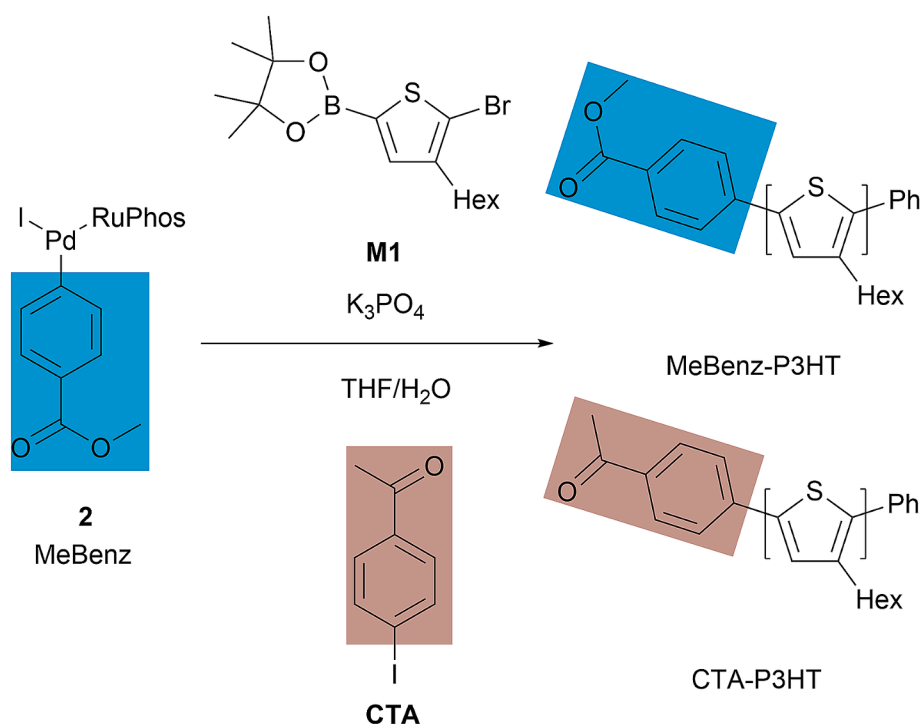
In the series without CTA (Table 1, P1-3), a clear trend emerges. Although the $\bar{M}_{n,\text{top}}$ is comparable across all three samples, the \bar{M}_n decreases with increasing water content. In the SEC spectra, the decrease in \bar{M}_n , especially from the sample with the highest water content **P1**, was primarily attributed to the presence of a shoulder on the right side at higher elution volumes (Fig. 2a). On the left side, there is also a small shoulder visible, and these two shoulders combined are revealing side reactions such as transfer reactions, deboration, dehalogenation and disproportionation, thereby impacting the \bar{M}_n .

Conversely, the second series with CTA presents the opposite trend (Error! Reference source not found., P4-6). Although the dispersity remains consistent, the \bar{M}_n and $\bar{M}_{n,\text{top}}$ of **P4** are higher than **P5** and **P6**, despite the presence of a shoulder on the right side of the SEC spectrum

Table 1

Influence of water content and the chain transfer agent (CTA) on the molar mass and dispersity of **P1-P6**. \bar{M}_n , $\bar{M}_{n,\text{top}}$ and dispersity (\bar{D}) are based on SEC data calibrated using polystyrene standards.

Sample	THF/ H_2O	CTA (mol%)	\bar{M}_n (kg/mol)	$\bar{M}_{n,\text{top}}$ (kg/mol)	\bar{D}
P1	10/1	0	3.3	6.9	1.58
P2	40/1	0	4.6	6.9	1.32
P3	60/1	0	4.9	7.1	1.29
P4	10/1	20	2.2	3.5	1.35
P5	40/1	20	1.9	2.5	1.39
P6	60/1	20	1.9	2.1	1.30



Scheme 2. SMCTCP of **M1** using external initiator **2** with and without the presence of a chain transfer agent (CTA), 4-iodoacetophenone. MeBenz = methyl benzoate, RuPhos = 2-dicyclohexylphosphino-2'-diisopropoxybiphenyl.

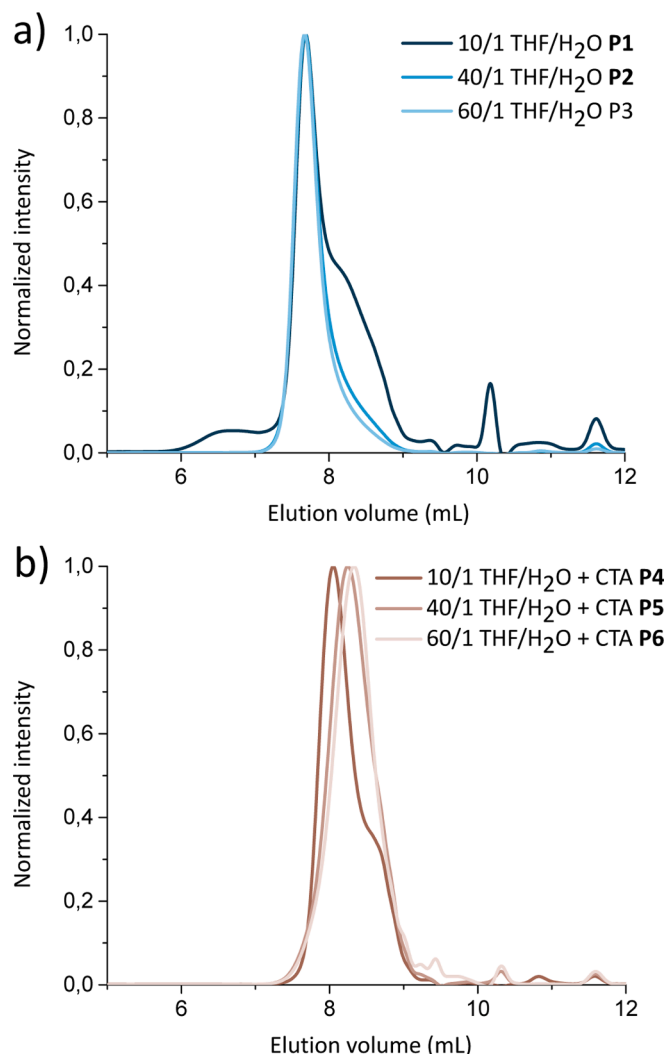


Fig. 2. SEC spectra of a) different amounts of water and b) having a different water content in the presence of 20 mol% chain transfer agent (CTA).

in the 10/1 THF/H₂O ratio sample (Fig. 2b). However, the \bar{M}_n noticeably decreases compared to samples without CTA, suggesting that intermolecular reactions are occurring. This is further confirmed by ¹H NMR spectra before Soxhlet extraction. In the absence of transfer reactions, only signals appearing from the methyl benzoate should be visible. In the case of transfer reactions, both methyl benzoate and CTA as end groups are present and the ratio of incorporated CTA-to-methyl benzoate is used to estimate the controlled character of the

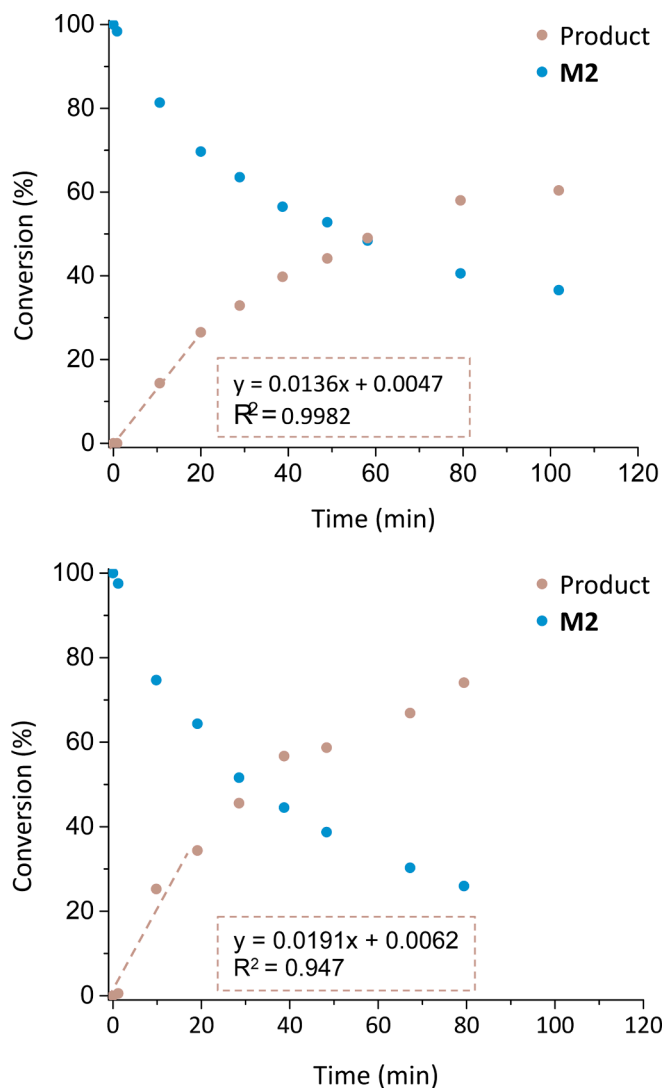
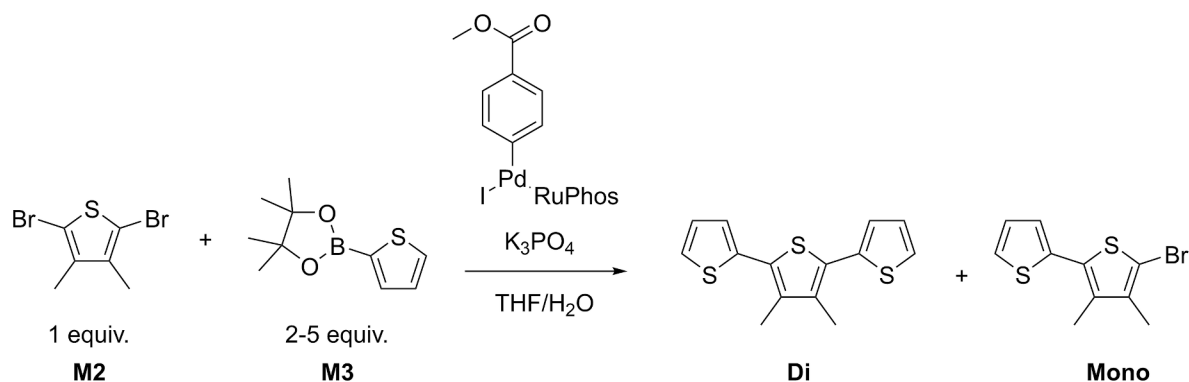


Fig. 3. Formation of product and disappearance of M2. Top) using 2 equivalents of M3. Bottom) using 5 equivalents of M3.

polymerization. In the ¹H spectra of all three samples polymerized with CTA, aromatic signals corresponding to both the methyl benzoate and the CTA are present, thus indicating transfer (SI S7, P4-6). Interestingly, the sample with the highest water content (P4, 10/1 THF/H₂O) has the lowest ratio of CTA-over-methyl benzoate, being equal to 0.29 compared to 1.26 and 1.20 for the 40:1 and 60:1 THF:H₂O ratios. A lower value indicates fewer transfer reactions and better control over the



Scheme 3. Model reaction for the investigation of the rate determining step, with M3 being varied from 2 to 5 equivalents.

end groups (SI S4). This proves that increasing water content reduces transfer reactions, although it also negatively impacts the polymerization process. This role of water in reducing transfer reactions is in line with the activation-deactivation mechanism during the Negishi polymerization. This polymerization is typically performed under moisture-free conditions, promoting transfer reactions which are known to occur approximately every four monomer insertions [27]. The precise role of water in the catalytic cycle remains to be elucidated, prompting an investigation into the rate-determining step, which may provide insights into where it comes into play.

2.3. Rate-determining step in the SMCTCP using a Pd(RuPhos) initiator

To investigate the rate-determining step in SMCTCP using the Pd (RuPhos) initiator, small molecule Suzuki-Miyaura model reactions, similar to the monomers employed in the polymerization process, are conducted. The reaction involves the coupling of one equivalent of 2,5-dibromo-3,4-dimethylthiophene **M2** with two equivalents of thiophene-2-boronic acid pinacol ester **M3** and monitoring the reaction progress over time using ^1H NMR (Scheme 3). To determine if the transmetalation (TM) step is the rate-determining step, the experiment is also repeated with five equivalents of **M3**. If TM is rate-limiting, increasing the concentration of **M3** should accelerate the reaction which can be monitored by the formation of mono- and di-reacted product.

Unlike the SMCTCPs, the model reaction is initiated by the addition of a base solution, allowing the measurements of a data point t_0 . Consequently, the amount of base used during these model reactions is lower than during the SMCTCPs due to solubility limitations. The conversion is measured by taking a fixed volume of the sample and adding it to an NMR tube containing 0.250 mL of THF- d_8 , while the amount of non-deuterated THF serves as the internal standard. The conversion is plotted as a function of time, focusing only on the initial slope. Upon comparing the initial slope of the reactions using two and five equivalents of **M3**, only a small difference in reaction rate is observed (Fig. 3): 0.0136 ± 0.0004 and 0.0191 ± 0.0032 for two and five equivalents, respectively. This modest rate difference does not align with the expected increase from a 2.5-fold increase of **M3** if TM were the rate-determining step. Then, the reaction rate should scale proportionally to $[\text{P}^*][\text{M}]$, meaning the rate would increase by a factor 2.5, assuming that just one monomer and the growing polymer chain participate in the TM. Accounting for standard errors, the rate difference diminishes even further, providing evidence that the TM is not the rate-determining step. Given these findings, the rate-determining step was speculated to be either oxidative addition (OA), reductive elimination (RE) or ring-walking (RW). OA is typically ruled out, as dialkyl biaryl monophosphines like RuPhos are generally associated with fast OA due to closer approaching of the aryl electrophile compared to $\text{L}_2\text{Pd}(0)$ complexes [31–33]. Thus, the rate-determining step in this context is more likely to be either RE or RW. It is hypothesized that water may stabilize the Pd(RuPhos)-polymer complex during RW, thus reducing the likelihood of transfer reactions. To mitigate the negative effects inherently related to water, different cosolvents are explored to interact with this complex without adversely affecting the polymerization.

2.4. Influence of cosolvents on SMCTCPs

To explore the impact of different cosolvents in mimicking the positive effects of water on transfer reactions and their involvement in the catalytic cycle, polymerizations are carried out using a 60/1 THF/ H_2O reaction mixture and replacing 10 vol% of THF with various cosolvents. The water content is reduced to minimize its direct influence during the polymerization while still ensuring intramolecular transfer and dissolving the base allowing for the formation of OH^- . The investigated cosolvents are divided into two groups: alcohol-based (Error! Reference source not found., P9-11) and aromatic compounds (Error! Reference source not found., P12-17) in addition to cosolvent-free

Table 2

Combination of all different cosolvents with and without extra chain transfer agents (CTA). $\bar{M}_{n, \text{top}}$ and dispersity (D) are based on SEC data using polystyrene standards.

Sample	Cosolvent	THF/ H_2O	CTA (mol%)	\bar{M}_n (kg/ mol)	$\bar{M}_{n, \text{top}}$ (kg/ mol)	D
P7	/	60/1	0	4.8	6.8	1.28
P8	/	60/1	20	1.6	2.9	1.56
P9	MeOH	60/1	0	4.4	6.7	1.34
P10	HexOH	60/1	0	5.0	7.7	1.36
P11	5-Hex-1-enol	60/1	0	0.5	1.4	1.98
P12	BA	60/1	0	1.7	2.0	1.42
P13	BN	60/1	0	3.4	4.9	1.56
P14	Toluene	60/1	0	4.6	6.5	1.28
P15	Anisole	60/1	0	4.9	7.0	1.29
P16	DMB	60/1	0	5.0	6.9	1.28
P17	Phenol	60/1	0	1.3	2.0	1.63
P18	HexOH	60/1	20	2.2	3.2	1.31
P19	Toluene	60/1	20	2.1	2.8	1.30
P20	Anisole	60/1	20	2.6	3.7	1.26
P21	DMB	60/1	20	2.4	2.9	1.27

MeOH = methanol, HexOH = hexanol, BA = benzaldehyde, BN = benzonitrile, DMB = 1,4-dimethoxybenzene.

reference samples **P7** and **P8** (with CTA).

Among the alcohol-based cosolvents, polymerization with methanol (**P9**) obtained a similar $\bar{M}_{n, \text{top}}$ compared to the sample without cosolvent (**P7**). However, the polymer solution becomes darker and more turbid which is likely due to the low solubility of the growing polymer in methanol. In contrast, using 1-hexanol (**P10**), which has a longer apolar alkyl chain, improves solubility. This results in an increased $\bar{M}_{n, \text{top}}$ that surpasses the $\bar{M}_{n, \text{top}}$ of **P7**. However, the dispersity also increases, from 1.28 to 1.36, echoing the effect of an increasing water content in the absence of CTA. When testing 5-hexen-1-ol as cosolvent, the double bond is expected to interact more readily with the Pd(RuPhos) complex. In **P11**, with 5-hexen-1-ol as cosolvent only yields oligomers, thereby showing a clear difference with 1-hexanol.

The aromatic cosolvents are expected to interact with the Pd (RuPhos) polymer complex, stabilizing and preventing it from dissociating during RW. Among the electron-poor cosolvents, no improvements are obtained as BA and BN (**P12** and **P13**, respectively) lead to a significant increase in dispersity and dramatical decrease of the $\bar{M}_{n, \text{top}}$. In contrast, polymerizations using more electron-rich cosolvents, such as toluene (**P14**), anisole (**P15**), and 1,4-dimethoxybenzene (**P16**) produce polymers with similar $\bar{M}_{n, \text{top}}$ values and dispersity values compared to **P7**. Phenol, despite being electron-rich and a combination of both classes, failed to produce a controlled polymerization. This could possibly be due to the formation of phenoxide-anions after reaction with K_3PO_4 which can induce side reactions, poison the Pd catalyst, interact with the boronic ester functionalities, altering monomer reactivity or causing degradation.

Next, cosolvents that achieved similar results compared to **P7** are polymerized again in the presence of 20 mol% CTA (Table 2, P18-21). When 1-hexanol (**P18**) is used as a cosolvent, the dispersity decreases compared to **P8**, while the $\bar{M}_{n, \text{top}}$ increases slightly. However, **P18** remains well below the values of polymers synthesized without CTA, revealing the presence of transfer reactions. This result is in line with the sample polymerized using an increased water content (Error! Reference source not found., **P4**). Overall, the amount of water can be reduced and can be mimicked by hexanol, but a controlled polymerization is still not obtained. Among the aromatic compounds, only anisole, 1,4-dimethoxybenzene and toluene are used in combination with 20 mol% of CTA. Toluene (**P19**), being the least electron-rich, results in the same $\bar{M}_{n, \text{top}}$, but with a lower dispersity compared to **P8**. 1,4-dimethoxybenzene (**P20**) produces similar results as **P8**, but with a reduced dispersity, while anisole (**P21**) results in a polymer with a small

Table 3

Influence extra RuPhos on the controlled behavior of the SMCTCP with and without CTA and cosolvent. The equivalents of RuPhos are compared to amount of Pd (RuPhos) initiator. \bar{M}_n , $\bar{M}_{n, top}$ and dispersity (\mathcal{D}) are based on SEC data using polystyrene standards.

Sample	RuPhos	Cosolvent	THF/H ₂ O	CTA (mol%)	\bar{M}_n (kg/mol)	$\bar{M}_{n, top}$ (kg/mol)	\mathcal{D}
P7	/	/	60/1	0	4.8	6.8	1.28
P8	/	/	60/1	20	1.6	2.9	1.56
P22	1.5 equiv.	/	60/1	0	5.5	6.8	1.16
P23	1.5 equiv.	/	60/1	20	6.0	8.0	1.24
P24	1.5 equiv.	HexOH	60/1	0	6.1	7.9	1.21
P25	1.5 equiv.	HexOH	60/1	20	5.0	6.5	1.20
P26	1.5 equiv.	Anisole	60/1	0	5.2	6.7	1.25
P27	1.5 equiv.	Anisole	60/1	20	4.3	6.1	1.28

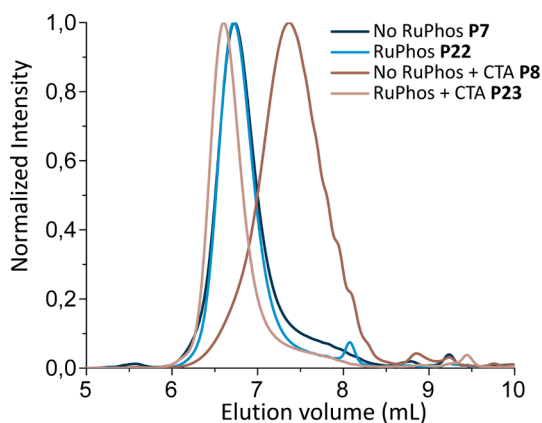


Fig. 4. SEC data of **P7-8** and **P22-23** synthesized with and without extra RuPhos in combination with and without chain transfer agent (CTA).

increased $\bar{M}_{n, top}$ and a reduced dispersity.

Following Soxhlet extraction, the polymer samples are analyzed using MALDI-ToF spectrometry to assess the presence of different end groups as this provides additional information regarding the controlled nature (SI S9). Aromatic cosolvents **P14-16** without CTA show end groups similar to those of **P7**, suggesting a comparable level of control. In contrast, **P10**, using 1-hexanol, exhibited a broader range of end groups, indicating less control which is again similar to **P1** having a higher water content. In polymerizations conducted with the combination of CTA and cosolvents, different observations are made. As explained before, the molar mass of these polymers is considerably lower due to the inability of cosolvents to prevent all transfer reactions. However, in **P18** and **P20** the amount of polymers with CTA as the end group is lower than in **P8**, while toluene and 1,4-dimethoxybenzene, yielding **P19** and **P21**, show negligible differences compared to **P8** (SI S10). These results show that cosolvents such as 1-hexanol and anisole can positively influence the SMCTCP, but the effect remains limited. In conclusion, the choice of cosolvents influences the controlled character in SMCTCPs and can be used to replace a portion of the water content, thereby potentially stabilizing the Pd(RuPhos)-polymer complex and improving the solubility. However, the selection of the right cosolvent is a delicate balance influenced by solubility, functional groups and electron density and no cosolvent is sufficient to gain full control over the SMCTCP.

2.5. Influence of extra RuPhos ligand on SMCTCP

A potential modification to the Pd(RuPhos) initiated SMCTCP involves the addition of additional RuPhos. Previous studies have shown that when a precatalyst, such as RuPhos Pd G3 is used to synthesize the initiator, more than one equivalent of RuPhos is typically employed. However, the effect of additional RuPhos equivalents has not yet been studied with an isolated Pd(RuPhos) initiator. Since each palladium

atom in the initiator already interacts with one RuPhos ligand, one could expect that additional RuPhos should not significantly influence the controlled nature of the polymerization. Nonetheless, research conducted by the group of Choi demonstrated that additional RuPhos in their *in-situ* formed initiator dramatically reduced the dispersity [25].

To investigate this further, similar polymerization with and without CTA are repeated, using an additional 1.5 equivalents of RuPhos. For comparison, the previously established benchmarks **P7** and **P8** are shown in Table 3. In the first SMCTCP conducted with extra ligand (**P22**), the $\bar{M}_{n, top}$ of this sample remains unchanged compared to **P7**, but the dispersity decreases from 1.28 to 1.16, representing a significant enhancement regarding the controlled character (Fig. 4, blue). Encouraged by this result, the polymerization is repeated with additional CTA. Despite the small amount of free ligand compared to the amount of cosolvent used in previous experiments, the result is striking. Comparing **P8** and **P23**, the $\bar{M}_{n, top}$ increases from 2.9 to 8.0 kg/mol, while the dispersity decreases from 1.56 to 1.24 (Fig. 4, brown). Notably, the $\bar{M}_{n, top}$ of **P23** is even higher than that of **P22**, an unexpected result which can only be explained by a weighing error of the Pd(RuPhos) initiator. Analysis by ¹H NMR, SEC and MALDI-ToF reveals no anomalies that can otherwise explain the higher molar mass. Using ¹H NMR, the ratios of CTA-over-methyl benzoate end groups can again be calculated to determine the amount of transfer reactions. In **P8** using 20 mol% of CTA and a 60/1 THF/H₂O, this ratio after purification is equal to 0.68 whereas for **P23** with extra RuPhos, the ratio decreases to 0.09, confirming the significant effect of the additional ligand.

Given the success of the extra free ligand, the next step is to combine cosolvents with RuPhos to further enhance the SMCTCP. Polymerizations are carried out with and without CTA, using hexanol (**P24-25**) or anisole (**P26-27**) as cosolvent, which had previously shown some improvement. However, for both cosolvents, the $\bar{M}_{n, top}$ and dispersity were similar to those in **P22** and **P23**. Combining cosolvent and RuPhos with CTA results in polymers with an improved $\bar{M}_{n, top}$ and decreased dispersity, but the effects are comparable to the polymer synthesized with only RuPhos and CTA, indicating that cosolvents do not offer additional advantage when extra RuPhos is already employed. These conclusions are supported by MALDI-ToF analysis of **P22-27**, compared to **P7** and **P8** (SI S9). In general, the samples without CTA are comparable, only **P22** without extra cosolvent shows fewer different end groups, and the methyl benzoate/phenyl end group combination is the only dominant signal. For CTA-based samples, the same conclusions apply, with the exception that the polymer **P27**, synthesized using anisole, has less CTA-based polymers in its spectrum.

Given the clear impact of RuPhos in enhancing the controlled character of the SMCTCP, further experiments are conducted to investigate the species present during polymerization using ³¹P NMR in the absence and presence of extra RuPhos. The influence of the different compounds, e.g. external initiator, ligand and base, is investigated first to determine if any interactions or new species are formed before the polymerization itself. Fig. 5 shows the ³¹P NMR spectrum of the external initiator **2** in d⁸-THF and D₂O, which displays a single signal at 23 ppm. When 1.5 equivalents of RuPhos are added, a second signal at -10 ppm appears,

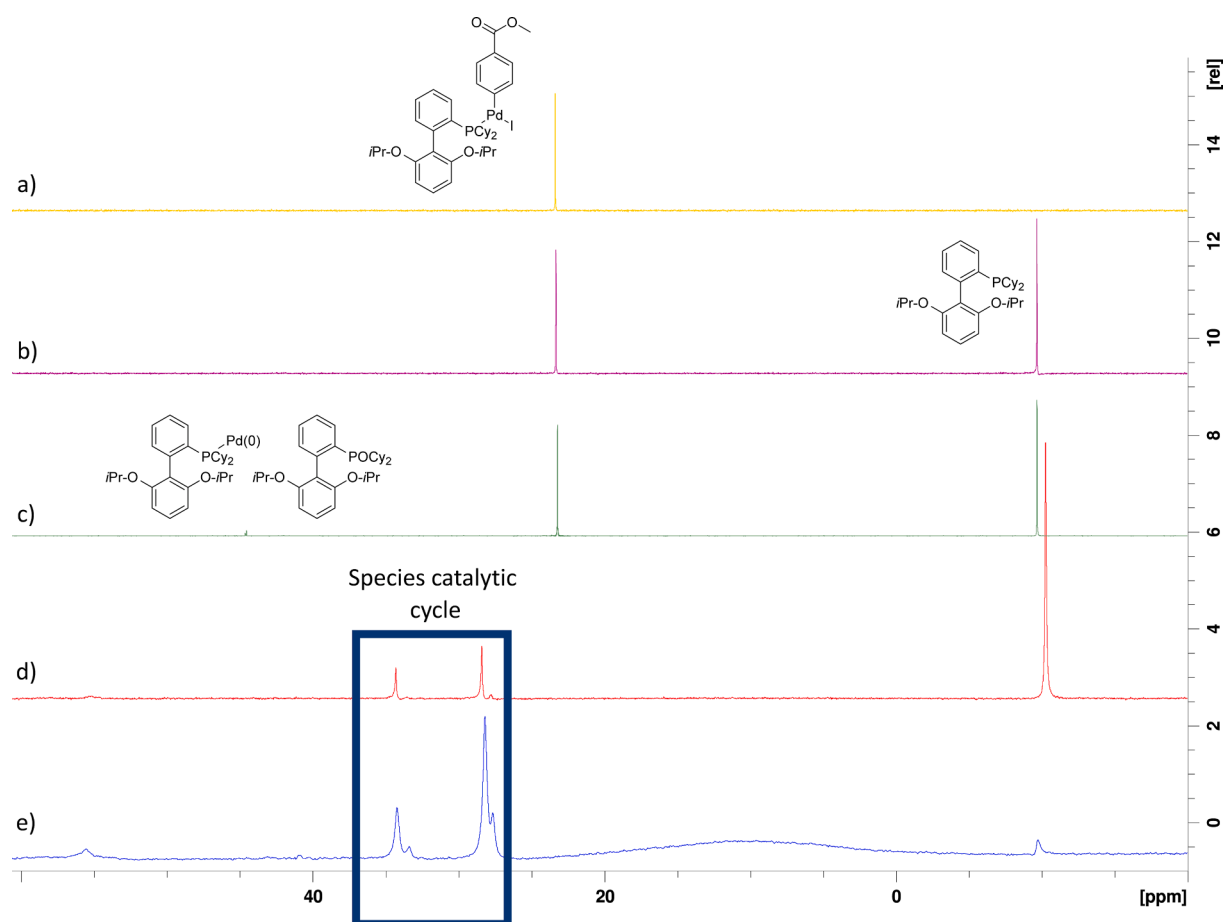


Fig. 5. ^{31}P NMR spectra of a) PdRuPhos initiator **2** in d^8 -THF and D_2O , b) PdRuPhos initiator + extra RuPhos, c) PdRuPhos + extra RuPhos + K_3PO_4 , d) SMCTCP with extra RuPhos and e) SMCTCP without extra RuPhos.

corresponding to the free RuPhos ligand. No other signals are observed, indicating that the formation of a $\text{Pd}(\text{RuPhos})_2$ species from the oxidatively inserted $(\text{Ar})\text{Pd}(\text{RuPhos})\text{-halide}$ complex is unlikely. After adding K_3PO_4 , the spectrum remains mostly unchanged, with the exception of a small signal at 44 ppm. This value can possibly be attributed to the formation of oxidized RuPhos, which might be formed by the oxidation of the external initiator or the formation of a $\text{Pd}(0)\text{RuPhos}$ particle [34,35]. K_3PO_4 itself is not visible, likely due to the solubility issues or phase separation of water and THF at high base concentrations.

To investigate the polymerization process itself, some modifications to the general procedure are necessary. The external initiator concentration is increased in order to be quantified by the NMR spectrometer. To achieve this, the volume of the THF/ D_2O reaction mixture is reduced to obtain a concentration of 0.2 M instead of 0.02 M. Additionally, the DP is also reduced in such a way as to increase the amount of initiator. The polymerization is performed with and without 1.5 equivalents of free RuPhos. Despite the suboptimal shimming of one of the samples due to the presence of insoluble inorganic compounds and water in the NMR tube, the comparison between the two spectra reveals that the sample without extra RuPhos contains a signal of free RuPhos. This indicates that at a certain point during the polymerization some of the initiator is destroyed, leading to an accumulation of free RuPhos over time, which may gradually start to stabilize the polymerization.

2.6. Computational study and hypothesis

Computations were performed at the B3LYP [36] /LANL2DZ level of theory. Within this methodology, the core electrons of the heavier atoms (10 per phosphorus or sulfur atom and 28 per palladium atom) are

treated using effective core potentials. Dispersion effects were treated with the D3 correction by Grimme including Becke-Johnson damping [37]. All calculations were performed using the Q-Chem software package [38]. To implicitly describe solvent effects, geometries were optimized using the SMD solvation model [39]. Frequency calculations were carried out using the SwiG-C-PCM solvation model [40,41] where atomic radii by Bondi [42] were used for all elements except hydrogen, for which a revised atomic radius [43] was employed. The solvent-accessible surface was constructed by using 194 Lebedev grid points on all atoms except for hydrogen, where 110 points were used.

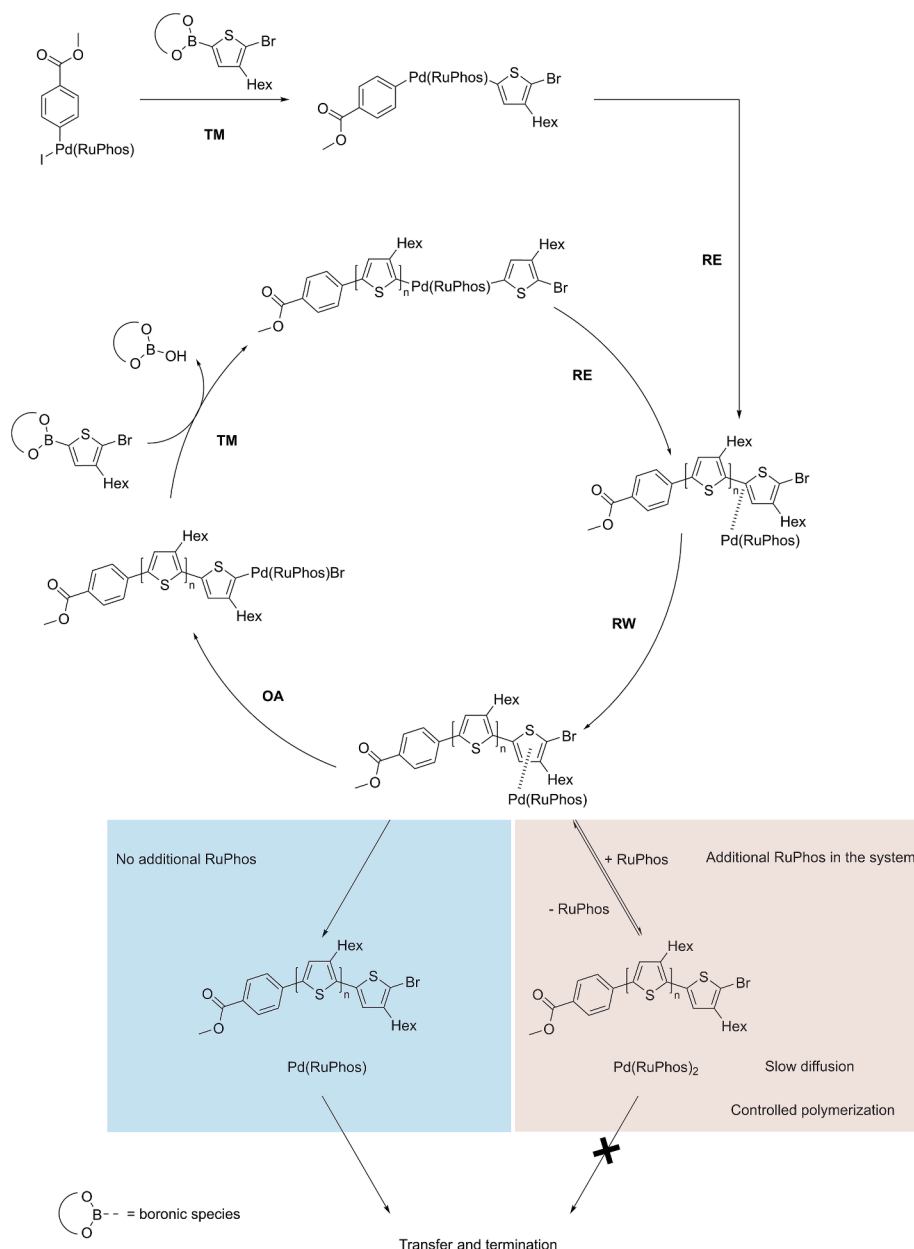
To investigate the stability of different complexes of palladium, the polymer chain, RuPhos, and the solvent THF, the free enthalpy of different species in equilibrium geometries was calculated and compared. In the resting phase after the reductive elimination and before the insertion into the C-Br bond, the catalyst coordinates the π system of the polythiophene. As a simplified equivalent of the polymer chain, 2,2'-bithiophene (Th_2) was studied. Such a complex is, in principle, stable towards dissociation, since the reaction



is endergonic. However, in the presence of the solvent, this reaction becomes more favorable due to the more efficient coordination of the palladium atom in a complex with THF.



It can be expected that the decoordination becomes even more favorable for a more extended polymer chain, as well as in the presence of sterically demanding sidechains or the electron-rich bromine



Scheme 4. Overall Suzuki-Miyaura CTCP mechanism, including the extra step during RW, with and without additional RuPhos.

substituent which is essential for the polymerization mechanism. However, the coordination of the palladium atom by a RuPhos molecule is more favourable than forming a complex with THF. If there is excess RuPhos in the solution, the dissociated palladium will form the Pd(RuPhos)₂ complex, which is confirmed computationally:



This complex is stable with respect to further dissociation due to the high binding energy between palladium and RuPhos:



This binding energy is not as high as the one corresponding to the interaction energy between a palladium atom with a single RuPhos molecule:



However, it is high enough to expect the intermediate formation of

Pd(RuPhos)₂ during the reaction in case of dissociation of the palladium-polymer bond.

These results, combined with the evidence of free ligand formation during the polymerization, suggest the following tentative hypothesis (Scheme 4). During RW, the Pd(RuPhos) complex can start to diffuse away from the growing polymer chain due to its relatively low binding energy. In the presence of additional RuPhos, when the Pd(RuPhos) diffuses away it forms Pd(RuPhos)₂, with the second ligand more weakly bound. This change significantly increases the size of the Pd species, hindering its diffusion and allowing its reintroduction into the growing polymer chain before transfer occurs. During polymerizations without additional RuPhos, the weakly bound Pd(RuPhos)-polymer complex lacks the availability of a second RuPhos ligand to slow down its diffusion. As a result, the catalyst may become available for transfer reactions, as supported by the reactions with CTA, or undergo degradation, indicated by the free RuPhos signal in the ³¹P NMR spectra. Over time, the increasing amount of free RuPhos improves in gaining control during the SMCTCP.

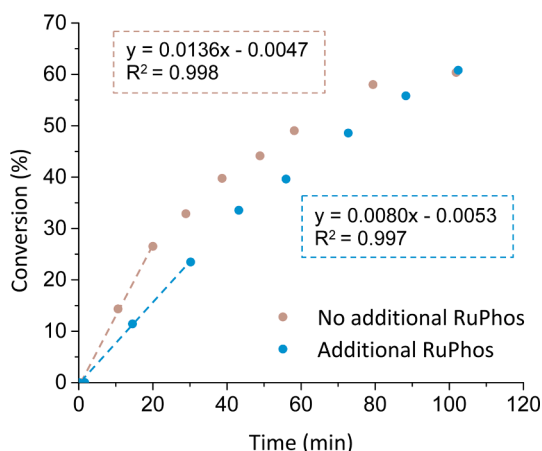


Fig. 6. Initial reaction rates of the model reactions with and without additional RuPhos.

In comparison, in a typical activation-deactivation-type of Negishi polymerization, the catalyst is allowed to diffuse away. This is not only due to the absence of water, but also due to a lack of free RuPhos allowing for efficient diffusion and inducing transfer reactions. In the SMCTCP, this is avoided due to the combined presence of both water and RuPhos, hence explaining the synergetic behavior leading to controlled behavior excluding transfer reactions. They allow for the formation of a solvent cage on the one hand and a temporary Pd(RuPhos)₂ formation on the other hand, minimizing effective transfer reactions.

As the strength of the complexation between the growing polymer backbone and the Pd(RuPhos) species is monomer dependent, the ratio of RuPhos-to-PdRuPhos needed to achieve a controlled behavior should be case specific as well. Based on literature from Choi *et al.* it becomes clear that this is indeed the case as the amount of RuPhos varies between 1.5 and 6 equivalents [24,28,30].

2.7. Reaction rate with and without RuPhos

Since the reversible binding of a second RuPhos ligand during RW is possible, the overall polymerization rate is expected to be lower in the presence of additional RuPhos, particularly in the initial stages of the reaction. To test this, the reaction rate is compared using the previously established model reaction with M2 and M3, with and without the presence of an additional 1.5 equivalents of RuPhos. In Fig. 6, the conversion as a function of time is visualized. The resulting graph reveals a clear difference in initial slopes, 0.0136 ± 0.0004 and 0.0080 ± 0.0003 , with and without additional RuPhos respectively, indicating distinct reaction rates at the start. Over time, however, the reaction rates start to become parallel and behave more similarly. This observation aligns with the proposed mechanism, where free RuPhos is gradually formed, enabling the temporary formation of Pd(RuPhos)₂, which influences the polymerization mechanism and reaction rate.

3. Conclusion

In summary, the influence of the amount of water on the transfer reaction during SMCTCP has been investigated, particularly in the presence of CTA. It has been found that a higher water content reduces the transfer reactions, which positively impacts the molar mass of the polymers. However, a controlled character is not achieved, as the higher water content also promotes side reactions and reduces solubility. Next, model reactions were conducted to gain insights into where exactly this water could impact the catalytic cycle. It was concluded that the TM cannot be the rate-determining step and that water should influence RW via stabilization of the growing Pd(RuPhos)-polymer complex. To mitigate the drawbacks of water, its amount was minimized and

cosolvents were added to mimic its positive effects. Based on SEC, ¹H NMR and MALDI-ToF analysis, cosolvents such as 1-hexanol and anisole do influence the controlled behavior to some extent, though no complete control is achieved. Ultimately, the addition of extra RuPhos ligand has been proven to be the crucial factor in achieving full control over the SMCTCP, as evidenced by a reduction of the dispersity from 1.28 to 1.16. Even in the presence of CTA, a controlled character was obtained as the molar mass of the obtained polymers is hardly affected. In conclusion, two main conditions should be met for the Pd(RuPhos) initiator to stick with one growing polymer chain and achieve a controlled SMCTCP: the presence of an optimal amount of water and the addition of excess RuPhos. Based on computational results, ³¹P NMR spectra, and the comparison in reaction rates with and without additional RuPhos, a plausible working mechanism for the role of additional RuPhos could be proposed. The Pd(RuPhos) catalyst is allowed to detach from the growing polymer chain during the polymerization process. However, the presence of additional RuPhos, either through degradation of Pd (RuPhos) or by its direct addition at the start of the polymerization, slows the reaction and hinders efficient diffusion. This occurs via the temporary formation of the bulky Pd(RuPhos)₂, which restricts diffusion and the related transfer reactions. Consequently, this mechanism enables the SMCTCP to exhibit a controlled behavior with the condition that additional RuPhos is present from the beginning. The combined presence of water and additional RuPhos introduces a stark and impactful difference with the activation-deactivation mechanism of the Negishi polymerization, where the catalyst detaches during the process. The presence of water (solvent cage) and extra RuPhos (hindered diffusion) in combination with different functional groups on the monomer explains why the same initiator system can behave differently across these two polymerization techniques.

Author Contributions

All authors have given approval to the final version of the manuscript. All authors significantly contributed to this research. S.D. was the main contributor to the investigation, the methodology and validation. S.D. conducted the visualization and writing of the original draft. F.M. and T.J. were responsible for the calculations and the written part of the manuscript regarding these calculations. P.G. and J.D.W. were responsible for the formal analysis and investigation off MALDI-ToF data. G.K. was responsible for conceptualization, funding acquisition, project administration, and supervision. All contributed evenly to the review and editing of writing this manuscript.

Funding Sources

Funding sources: 1SB1623N.
Infrastructure grant: I002720N.

CRediT authorship contribution statement

Siebe Detavernier: Writing – original draft, Investigation, Data curation. **Florian Matz:** Writing – review & editing, Data curation. **Julien De Winter:** Writing – review & editing, Data curation. **Pascal Gerbaux:** Writing – review & editing, Data curation. **Thomas Jagau:** Writing – review & editing, Supervision. **Guy Koeckelberghs:** Writing – review & editing, Funding acquisition, Conceptualization.

Declaration of competing interest

The authors declare that they have no known competing financial interests or personal relationships that could have appeared to influence the work reported in this paper.

Acknowledgment

This research was funded by the Fund for Scientific Research (FWO-Flanders - 15B1623N) and by Onderzoeksfonds KU Leuven/Research Fund KU Leuven. S.D. is doctoral fellow of the Fund for Scientific Research (FWO-Flanders).

This research was supported by the Research Foundation Flanders (FWO) through infrastructure grant I002720N.

I acknowledge the use of ChatGPT to identify improvements in the writing style.

Appendix A. Supplementary material

Supplementary data to this article can be found online at <https://doi.org/10.1016/j.eurpolymj.2025.113951>.

Data availability

Data will be made available on request.

References

- [1] T.M. Swager, 50th anniversary perspective: conducting/semiconducting conjugated polymers a personal perspective on the past and the future, *Macromolecules* 50 (2017) 4867–4886, <https://doi.org/10.1021/ACS.MACROMOL.7B00582>.
- [2] A. Facchetti, π -Conjugated polymers for organic electronics and photovoltaic cell applications, *Chem. Mater.* 23 (2011) 733–758, <https://doi.org/10.1021/CM102419Z>.
- [3] P.M. Beaujuge, J.M.J. Fréchet, Molecular design and ordering effects in π -functional materials for transistor and solar cell applications, *J. Am. Chem. Soc.* 133 (2011) 20009–20029, <https://doi.org/10.1021/JA2073643>.
- [4] S.W. Thomas, G.D. Joly, T.M. Swager, Chemical sensors based on amplifying fluorescent conjugated polymers, *Chem. Rev.* 107 (2007) 1339–1386, <https://doi.org/10.1021/cr0501339>.
- [5] C. Zhu, L. Liu, Q. Yang, F. Lv, S. Wang, Water-soluble conjugated polymers for imaging, diagnosis, and therapy, *Chem. Rev.* 112 (2012) 4687–4735, <https://doi.org/10.1021/cr200263w>.
- [6] H.-A. Ho, A. Najari, M. Leclerc, Optical detection of DNA and proteins with cationic polythiophenes, *Acc. Chem. Res.* 41 (2008) 168–178, <https://doi.org/10.1021/ar700115t>.
- [7] T.N. Nguyen, V.D. Phung, V. Van Tran, Recent advances in conjugated polymer-based biosensors for virus detection, *Biosensors* 13 (2023) 586, <https://doi.org/10.3390/BIOS13060586>.
- [8] A. Van Oosten, C. Verduyck, J. De Winter, P. Gerbaux, G. Koeckelberghs, Influence of the dispersity and molar mass distribution of conjugated polymers on the aggregation type and subsequent chiral expression, *Soft Matter* 19 (2023) 3794–3802, <https://doi.org/10.1039/D3SM00163F>.
- [9] H.S. Yang, H.N. Choi, I.H. Lee, Recent progress on end-group chemistry of conjugated polymers based on Suzuki-Miyaura catalyst-transfer polymerization, *Giant* 14 (2023) 100152, <https://doi.org/10.1016/J.GIANT.2023.100152>.
- [10] P. Willot, J. Steverlyncx, D. Moerman, P. Leclère, R. Lazzaroni, G. Koeckelberghs, Poly(3-alkylthiophene) with tuneable regioregularity: synthesis and self-assembling properties, *Polym. Chem.* 4 (2013) 2662–2671, <https://doi.org/10.1039/C3PY00236E>.
- [11] B. Timmermans, Y. De Coene, A. Van Oosten, K. Clays, T. Verbiest, G. Koeckelberghs, Influence of the irregularity of the molecular structure on the chiral expression of poly(fluorene)s, *Macromolecules* 55 (2022) 8303–8310, <https://doi.org/10.1021/ACS.MACROMOL.2C00234>.
- [12] C.R. Bridges, M.J. Ford, E.M. Thomas, C. Gomez, G.C. Bazan, R.A. Segalman, Effects of side chain branch point on self assembly, structure, and electronic properties of high mobility semiconducting polymers, *Macromolecules* 51 (2018) 8597–8604, <https://doi.org/10.1021/ACS.MACROMOL.8B01906>.
- [13] A. Yokoyama, T. Yokozawa, Converting step-growth to chain-growth condensation polymerization, *Macromolecules* 40 (2007) 4093–4101, <https://doi.org/10.1021/MA061357B>.
- [14] S. Ye, V. Lotocki, H. Xu, D.S. Seferos, Group 16 conjugated polymers based on furan, thiophene, selenophene, and tellurophene, *Chem. Soc. Rev.* 51 (2022) 6442–6474, <https://doi.org/10.1039/D2CS00139J>.
- [15] M.C. D'Alterio, È. Casals-Cruañas, N.V. Tzouras, G. Talarico, S.P. Nolan, A. Poater, Mechanistic aspects of the palladium-catalyzed suzuki-miyaura cross-coupling reaction, *Chem. A Eur. J.* 27 (2021) 13481–13493, <https://doi.org/10.1002/CHEM.202101880>.
- [16] E. Elmalem, A. Kiriy, W.T.S. Huck, Chain-growth suzuki polymerization of n-type fluorene copolymers, *Macromolecules* 44 (2011) 9057–9061, <https://doi.org/10.1021/MA201934Q>.
- [17] A. Yokoyama, H. Suzuki, Y. Kubota, K. Ohuchi, H. Higashimura, T. Yokozawa, Chain-growth polymerization for the synthesis of polyfluorene via Suzuki Miyaura coupling reaction from an externally added initiator unit, *J. Am. Chem. Soc.* 129 (2007) 7236–7237, <https://doi.org/10.1021/JA070313V>.
- [18] R. Nitto, Y. Ohta, T. Yokozawa, Suzuki-miyaura catalyst-transfer condensation polymerization for the synthesis of polyphenylene with ester side chain by using stable, reactive 1,1,2,2-tetraethylethylene glycol boronate (B(Epin)) monomer, *Macromolecules* 57 (2024) 985–990, <https://doi.org/10.1021/ACS.MACROMOL.3C02003>.
- [19] C. Amatore, A. Jutand, G. Le Duc, Kinetic data for the transmetalation/reductive elimination in palladium-catalyzed suzuki-miyaura reactions: unexpected triple role of hydroxide ions used as base, *Chem. – A Eur. J.* 17 (2011) 2492–2503, <https://doi.org/10.1002/CHEM.201001911>.
- [20] A.J.J. Lennox, G.C. Lloyd-Jones, Transmetalation in the Suzuki–Miyaura coupling: the fork in the trail, *Angew. Chem. Int. Ed.* 52 (2013) 7362–7370, <https://doi.org/10.1002/ANIE.201301737>.
- [21] C.F.R.A.C. Lima, A.S.M.C. Rodrigues, V.L.M. Silva, A.M.S. Silva, L.M.N.B.F. Santos, Role of the base and control of selectivity in the suzuki-miyaura cross-coupling reaction, *Chem. Cat. Chem.* 6 (2014) 1291–1302, <https://doi.org/10.1002/CCTC.201301080>.
- [22] K. Kosaka, Y. Ohta, T. Yokozawa, K. Kosaka, Y. Ohta, T. Yokozawa, Influence of the boron moiety and water on suzuki-miyaura catalyst-transfer condensation polymerization, *Macromol. Rapid Commun.* 36 (2015) 373–377, <https://doi.org/10.1002/MARC.201400530>.
- [23] J. Lee, H. Kim, H. Park, T. Kim, S.-H. Hwang, D. Seo, T. Dong Chung, T.-L. Choi, Universal Suzuki–Miyaura catalyst-transfer polymerization for precision synthesis of strong donor/acceptor-based conjugated polymers and their sequence engineering, *J. Am. Chem. Soc.* 143 (2021) 11180–11190, <https://doi.org/10.1021/jacs.1c05080>.
- [24] H. Kim, J. Lee, T. Kim, M. Cho, T.-L. Choi, Precision synthesis of various low-bandgap donor-acceptor alternating conjugated polymers via living suzuki-miyaura catalyst-transfer polymerization, *Angew. Chem. Int. Ed.* 61 (2022) e202205828, <https://doi.org/10.1002/anie.202205828>.
- [25] K.B. Seo, I.H. Lee, J. Lee, I. Choi, T.L. Choi, A rational design of highly controlled suzuki-miyaura catalyst-transfer polycondensation for precision synthesis of polythiophenes and their block copolymers: marriage of palladacycle precatalysts with MIDA-boronates, *J. Am. Chem. Soc.* 140 (2018) 4335–4343, <https://doi.org/10.1021/JACS.7B13701>.
- [26] M. Verswyvel, P. Verstappen, L. De Cremer, T. Verbiest, G. Koeckelberghs, Development of a universal chain-growth polymerization protocol of conjugated polymers: toward a variety of all-conjugated block-copolymers, *J. Polym. Sci. A Polym. Chem.* 49 (2011) 5339–5349, <https://doi.org/10.1002/POLA.25014>.
- [27] M. Verswyvel, J. Steverlyncx, S. Hadj Mohamed, M. Trabelsi, B. Champagne, G. Koeckelberghs, All-conjugated ABC-block-copolymer formation with a varying sequence via an unassociated catalyst, *Macromolecules* 47 (2014) 4668–4675, <https://doi.org/10.1021/MA500610P>.
- [28] J. Lee, H. Ryu, S. Park, M. Cho, T.L. Choi, Living Suzuki-Miyaura catalyst-transfer polymerization for precision synthesis of length-controlled armchair graphene nanoribbons and their block copolymers, *J. Am. Chem. Soc.* 145 (2023) 15488–15495, <https://doi.org/10.1021/JACS.3C04130>.
- [29] S.J. Firsan, V. Sivakumar, T.J. Colacot, Emerging trends in cross-coupling: twelve-electron-based L1Pd(0) catalysts, their mechanism of action, and selected applications, *Chem. Rev.* 122 (2022) 16983–17027, <https://doi.org/10.1021/ACS.CHEMREV.2C00204>.
- [30] J. Lee, H. Kim, H. Park, T. Kim, S.H. Hwang, D. Seo, T.D. Chung, T.L. Choi, Universal suzuki-miyaura catalyst-transfer polymerization for precision synthesis of strong donor/acceptor-based conjugated polymers and their sequence engineering, *J. Am. Chem. Soc.* 143 (2021) 11180–11190, <https://doi.org/10.1021/JACS.1C05080>.
- [31] B.T. Ingoglia, C.C. Wagen, S.L. Buchwald, Biaryl monophosphine ligands in palladium-catalyzed C–N coupling: an updated User's guide, *Tetrahedron* 75 (2019) 4199–4211, <https://doi.org/10.1016/J.TET.2019.05.003>.
- [32] B.P. Fors, D.A. Watson, M.R. Biscoe, S.L. Buchwald, A highly active catalyst for Pd-catalyzed amination reactions: cross-coupling reactions using aryl mesylates and the highly selective monoarylation of primary amines using aryl chlorides, *J. Am. Chem. Soc.* 130 (2008) 13552–13554, <https://doi.org/10.1021/JA8055358>.
- [33] M.R. Biscoe, B.P. Fors, S.L. Buchwald, A new class of easily activated palladium precatalysts for facile C–N cross-coupling reactions and the low temperature oxidative addition of aryl chlorides, *J. Am. Chem. Soc.* 130 (2008) 6686–6687, <https://doi.org/10.1021/JA801137K>.
- [34] S.O. Sotnik, A.M. Mishchenko, E.B. Rusanov, A.V. Kozytskiy, K.S. Gavrilenko, S. V. Ryabukhin, D.M. Volochnyuk, S.V. Kolotilov, Third generation buchwald precatalysts with XPhos and RuPhos: multigram scale synthesis, solvent-dependent isomerization of XPhos Pd G3 and quality control by 1H- and 31P-NMR spectroscopy, *Molecules* 26 (2021) 3507, <https://doi.org/10.3390/MOLECULES26123507>.
- [35] T.E. Barder, S.L. Buchwald, Rationale behind the resistance of dialkylbiaryl phosphines toward oxidation by molecular oxygen, *J. Am. Chem. Soc.* 129 (2007) 5096–5101, <https://doi.org/10.1021/JA0683180>.
- [36] J. Tirado-Rives, W.L. Jorgensen, Performance of B3LYP density functional methods for a large set of organic molecules, *J. Chem. Theory Comput.* 4 (2008) 297–306, <https://doi.org/10.1021/CT700248K>.
- [37] S. Grimme, A. Hansen, J.G. Brandenburg, C. Bannwarth, Dispersion-corrected mean-field electronic structure methods, *Chem. Rev.* 116 (2016) 5105–5154, <https://doi.org/10.1021/ACS.CHEMREV.5B00533>.
- [38] E. Epifanovsky, A.T.B. Gilbert, X. Feng, J. Lee, Y. Mao, N. Mardirossian, P. Pokhilko, A.F. White, M.P. Coons, A.L. Dempwolff, Z. Gan, D. Hait, P.R. Horn, L. D. Jacobson, I. Kaliman, J. Kussmann, A.W. Lange, K.U. Lao, D.S. Levine, J. Liu, S.

- C. McKenzie, A.F. Morrison, K.D. Nanda, F. Plasser, D.R. Rehn, M.L. Vidal, Z. Q. You, Y. Zhu, B. Alam, B.J. Albrecht, A. Aldossary, E. Alguire, J.H. Andersen, V. Athavale, D. Barton, K. Begam, A. Behn, N. Bellonzi, Y.A. Bernard, E.J. Berquist, H.G.A. Burton, A. Carreras, K. Carter-Fenk, R. Chakraborty, A.D. Chien, K. D. Closser, V. Cofer-Shabica, S. Dasgupta, M. De Wergifosse, J. Deng, M. Diedenhofen, H. Do, S. Ehlert, P.T. Fang, S. Fatehi, Q. Feng, T. Friedhoff, J. Gayvert, Q. Ge, G. Gidofalvi, M. Goldey, J. Gomes, C.E. González-Espinoza, S. Gulania, A.O. Gunina, M.W.D. Hanson-Heine, P.H.P. Harbach, A. Hauser, M. F. Herbst, M. Hernández Vera, M. Hodecker, Z.C. Holden, S. Houck, X. Huang, K. Hui, B.C. Huynh, M. Ivanov, Á. Jász, H. Ji, H. Jiang, B. Kaduk, S. Kähler, K. Khistyayev, J. Kim, G. Kis, P. Klunzinger, Z. Koczor-Benda, J.H. Koh, D. Kosenkov, L. Koulias, T. Kowalczyk, C.M. Krauter, K. Kue, A. Kunitsa, T. Kus, I. Ladjánszki, A. Landau, K.V. Lawler, D. LeFrancis, S. Lehtola, R.R. Li, Y.P. Li, J. Liang, M. Liebenthal, H.H. Lin, Y.S. Lin, F. Liu, K.Y. Liu, M. Loipersberger, A. Luenser, A. Manjanath, P. Manohar, E. Mansoor, S.F. Manzer, S.P. Mao, A. V. Marenich, T. Markovich, S. Mason, S.A. Maurer, P.F. McLaughlin, M.F.S. J. Menger, J.M. Mewes, S.A. Mewes, P. Morgante, J.W. Mullinax, K.J. Oosterbaan, G. Paran, A.C. Paul, S.K. Paul, F. Pavošević, Z. Pei, S. Prager, E.I. Proynov, Á. Rák, E. Ramos-Cordoba, B. Rana, A.E. Rask, A. Rettig, R.M. Richard, F. Rob, E. Rossomme, T. Scheele, M. Scheurer, M. Schneider, N. Sergueev, S.M. Sharada, W. Skomorowski, D.W. Small, C.J. Stein, Y.C. Su, E.J. Sundstrom, Z. Tao, J. Thirman, G.J. Tornai, T. Tsuchimochi, N.M. Tubman, S.P. Veccham, O. Vydrov, J. Wenzel, J. Witte, A. Yamada, K. Yao, S. Yeganeh, S.R. Yost, A. Zech, I.Y. Zhang, X. Zhang, Y. Zhang, D. Zuev, A. Aspuru-Guzik, A.T. Bell, N.A. Besley, K.B. Bravaya, B.R. Brooks, D. Casanova, J. Da Chai, S. Coriani, C.J. Cramer, G. Cserey, A. E. DePrince, R.A. Distasio, A. Dreuw, B.D. Dunietz, T.R. Furlani, W.A. Goddard, S. Hammes-Schiffer, T. Head-Gordon, W.J. Hehre, C.P. Hsu, T.C. Jagau, Y. Jung, A. Klamt, J. Kong, D.S. Lambrecht, W. Liang, N.J. Mayhall, C.W. McCurdy, J. B. Neaton, C. Ochsenfeld, J.A. Parkhill, R. Peverati, V.A. Rassolov, Y. Shao, L. V. Slipchenko, T. Stauch, R.P. Steele, J.E. Subotnik, A.J.W. Thom, A. Tkatchenko, D.G. Truhlar, T. Van Voorhis, T.A. Wesolowski, K.B. Whaley, H.L. Woodcock, P. M. Zimmerman, S. Faraji, P.M.W. Gill, M. Head-Gordon, J.M. Herbert, A.I. Krylov, Software for the frontiers of quantum chemistry: an overview of developments in the Q-Chem 5 package, *J Chem Phys* 155 (2021) 084801, <https://doi.org/10.1063/5.0055522>.
- [39] A.V. Marenich, C.J. Cramer, D.G. Truhlar, Universal solvation model based on solute electron density and on a continuum model of the solvent defined by the bulk dielectric constant and atomic surface tensions, *J. Phys. Chem. B* 113 (2009) 6378–6396, <https://doi.org/10.1021/JP810292N>.
- [40] M. Cossi, N. Rega, G. Scalmani, V. Barone, Energies, structures, and electronic properties of molecules in solution with the C-PCM solvation model, *J. Comput. Chem.* 24 (2003) 669–681, <https://doi.org/10.1002/JCC.10189>.
- [41] A.W. Lange, J.M. Herbert, Polarizable continuum reaction-field solvation models affording smooth potential energy surfaces, *J. Phys. Chem. Lett.* 1 (2010) 556–561, <https://doi.org/10.1021/JZ900282C>.
- [42] A. Bondi, Van der waals volumes and radii, *J. Phys. Chem.* 68 (1964) 441–451, <https://doi.org/10.1021/J100785A001/ASSET/J100785A001.FP.PNG.V03>.
- [43] R.S. Rowland, R. Taylor, Intermolecular Nonbonded Contact Distances in Organic Crystal Structures: Comparison with Distances Expected from van der Waals Radii, (1996). <https://doi.org/10.1021/JP953141>.